NASA Technical Memorandum 100082

High-Speed Flow Calculations Past 3-D Configurations Based on the Reynolds Averaged Navier-Stokes Equations

Denny S. Chaussee

March 1988

NASA
National Aeronautics and Space Administration

NASA Technical Memorandum 100082

High-Speed Flow Calculations Past 3-D Configurations Based on the Reynolds Averaged Navier-Stokes Equations

Denny S. Chaussee, Ames Research Center, Moffett Field, California

March 1988

National Aeronautics and
Space Administration

Ames Research Center
Moffett Field, California 94035

SUMMARY

A computational fluid dynamics tool has been developed that is capable of analyzing the viscous supersonic/hypersonic flow about realistic configurations. This technique can predict the flow in regions of canopies, wings, and canards in addition to the usual simple symmetric configurations. It also allows for interactions between aerodynamic surfaces such as the vortex interaction between canards and wings.

INTRODUCTION

The NASA Ames Parabolized Navier-Stokes (PNS) code was used as the mainline procedure to numerically simulate the viscous high-speed flow over these generic configurations. The parabolized approximation to the Navier-Stokes equations assumes that the flow is supersonic in the streamwise direction, and that the subsonic flow in the viscous sublayer is always positive in the streamwise direction. Thus, flows with large streamwise separation and flow reversals are excluded from treatment under the foregoing assumptions. However, crossflow separations are permitted.

Under these assumptions, the Navier-Stokes equations become parabolic in the streamwise direction, enabling a marching-solution procedure, which is computationally desirable and efficient. The form that is presented here was developed by Schiff and Steger (ref. 1). The turbulence model that has been used in this project is the Baldwin-Lomax model (ref. 2). The boundary conditions are the usual viscous no-slip at the wall, and a characteristic procedure is used to fit the bow shock wave which is the outermost boundary. Since the equations are cast in conservation-law form, all discontinuities within the flow domain are predicted accurately. Because of the possible complex nature of the configuration at each axial location as one proceeds down the body, an elliptic grid generator is employed to discretize the flow domain. Body shapes that have been marched over by the present algorithm include pointed cones (ref. 3), sphere-cones (ref. 4), three-dimensional reentry vehicles (refs. 4-6), an ogive-cylinder-boattail (ref. 7), a delta-wing configuration (ref. 8), the X-24 lifting body (ref. 5), the Space Shuttle (ref. 9), finned configurations (refs. 3 and 10), and, most recently, a generic fighter configuration (refs. 11 and 12). A representative number of these results are included in the present work.

GOVERNING EQUATIONS

The governing equations in the two base coordinate systems are transformed under a generalized coordinate mapping

$$\xi = \xi(a)$$

$$\eta = \eta(a,b,c)$$

$$\zeta = \zeta(a,b,c)$$

where the system (a,b,c) is either the Cartesian or the cylindrical coordinate system. The surface $\zeta = 0$ is the body surface, and a ζ = constant surface is the outer boundary or the bow shock surface. Since the solution is marched along the axial direction, a, the ξ = constant surface is chosen to be the axis-normal crossflow plane; therefore, ξ is not a function of b or c.

By invoking these approximations, the normalized Reynolds averaged Navier-Stokes equations transform under the generalized mapping as follows:

$$\frac{\partial \hat{E}}{\partial \xi} + \frac{\partial \hat{F}}{\partial \eta} + \frac{\partial \hat{G}}{\partial \zeta} + \hat{S} = \frac{1}{Re} \frac{\partial \hat{G}_v}{\partial \zeta} + \hat{S}_v$$

The vectors E, F, and G represent the inviscid flux vectors in the three transformed directions and can be found in reference 1.

BOUNDARY CONDITIONS

Boundary conditions must be applied at: (1) an initial plane of data at ξ = constant, (2) both extremes of the computational domain in the ζ-coordinate, and (3) at two places of data in the circumferential (η) direction (unless periodic).

An accurate initial data solution is needed. The parabolized Navier-Stokes prediction procedure can generate its own appropriate starting solution for conical bodies, or it can be started from a time dependent blunt-body program.

The boundary conditions specified at the surface of the body always include the no-slip and no-blowing conditions. Options are available that allow specifications of either an assigned wall temperature or an adiabatic wall condition.

For symmetric bodies at zero angle of yaw, the symmetry conditions in the $\eta = 0$ and $\eta = \eta_{max}$ planes are imposed. Otherwise, periodic boundary conditions are imposed in η.

The outer boundary of the computational domain is either specified as a known free stream or as the peripheral bow shock which is determined as the solution is marched downstream. Shock-fitting logic is used in the latter case.

NUMERICAL METHOD

The algorithm used in the present work is based on the Beam-Warming delta form as applied by Schiff and Steger (ref. 1). It is first- or second-order accurate in the marching direction and second-order accurate in the spatial directions. A fourth-order dissipation term is appended to the algorithm as well as an implicit smoothing term to further enhance the stability.

GENERATION OF COMPUTATIONAL GRIDS

The grid-generation process must achieve several ends that include: (1) developing accurate surface representations; (2) distributing points on the body surface; and (3) generating a clustered, well-ordered, smoothly varying, interior mesh. The configurations of current interest have only moderate variations in the axial direction, which simplifies problems associated with grid generation. In general, surface-conforming grids are required to simplify application of boundary conditions and to minimize the errors inherent in the thin-layer approximation. Such errors will be kept to a minimum by having the η = constant lines coincide with the important velocity and temperature gradients occurring within the flow. It is especially important to make sure the η = constant lines do not intercept the body at highly skewed angles.

RESULTS

A number of different results are presented which show the diversity of the PNS code. The flow regimes vary from a Mach number of 2 up to 14. Both laminar and turbulent flows have been considered as well as varying angles of attack. Configurations vary from simple cone-type bodies to lifting winged bodies such as the Space Shuttle or the generic supersonic cruise fighter.

The first case to be considered is the laminar hypersonic flow over a 30% blunt cone with a 5.6° cone half-angle. The free stream Mach number is 14.2; the Reynolds number is 0.62×10^6/ft; the ratio of wall temperature to the stagnation temperature is 0.29; and the angle of attack is 18°.

Figure 1 shows a comparison of the local separation line as obtained from the experiments (ref. 13) and calculations. The experimental separation line location was determined using the oil-flow technique. Two attachment lines (defined as the

lines from which the skin-friction lines diverge) coincide with the leeward and the windward meridians. In the experiment there was no evidence of any singular points at which the axial shear stress is zero.

To verify the capability of the present computer code in calculating the flow-field surrounding an MRV, a systematic study was undertaken. The configuration studied is a 14°/7° biconic vehicle as shown in figure 2, with nose blunting (R_N = 0.5) and slices on the windward and leeward sides. Results are presented for M_∞ = 10, α = 10°, Tw = 560° R, and turbulent flow with Re = 304,800/m.

In figure 3, a necessary comparison, the pitot-pressure variation through the shock layer at a specified x-station on the vehicle, is presented for experimental, inviscid, and laminar flow results. Good agreement between the calculated laminar results and the experimental data is apparent.

Figure 4 presents a comparison between the experimental and calculated heat transfer rates on the ϕ = 90 and the ϕ = 180 (lee side) meridians. The slight discrepancies are most likely due to a problem with predicting flow transition between laminar and turbulent flow.

Another complex configuration is the Space Shuttle orbiter. Numerical results have been obtained for the following wind-tunnel conditions: M_∞ = 7.9, α = 25°, Twall = 540° R, Re = 60,728/in. turbulent flow.

The three-dimensional solution was then obtained by marching downstream using the elliptic grid generator to construct the grid between the body and the fitted outermost shock wave. The grid consisted of either 61 or 121 points in the meridional direction and 45 geometrically stretched radial points. An example of the grid at an X/L = 0.66 is shown in figure 5. The outermost grid line is the bow wave, which is fitted using an implicit technique.

The computer-generated particle paths of figure 6 exhibit the main features of the flow field which surrounds the Shuttle. Two distinct phenomena are the vortices on the lee side of the body and the vortice caused by strake-wing.

Finally, a generic supercruise fighter configuration is considered. Numerical results for supersonic cruise at M_∞ = 2.169 are presented. The wind-tunnel conditions considered are such that the Reynolds number is turbulent. Adiabatic wall conditions are assumed at the body's surface, and an angle of attack of 4° is considered.

A numerical result for M_∞ = 2.2 flow past a wing-fuselage-nacelle has been completed. In figure 7, Cp distributions for some representative cross sections are presented. The solid line corresponds to a wing-fuselage result, the open symbols correspond to a wing-fuselage-nacelle result, and a solid symbol corresponds to experimental results.

REFERENCES

1. Schiff, L. B.; and Steger, J. L.: Numerical Simulation of Steady Supersonic Viscous Flows. NASA TP-1749, 1981.

2. Baldwin, B. S.; and Lomax, H. L.: Thin Layer Approximation and Algebraic Model for Separated Turbulent Flows. AIAA Paper 78-257, 1978.

3. Rai, M. M.; and Chaussee, D. S.: New Implicit Boundary Procedures: Theory and Application. AIAA Paper 83-0123, 1983.

4. Rizk, Y. M.; Chaussee, D. S.; and McRae, D. S.: Computation of Hypersonic Flow around Three-Dimensional Bodies at High Angles of Attack. AIAA Paper 81-1261, 1981.

5. Chaussee, D. S.; Patterson, J. L.; Kutler, P.; Pulliam, T. H.; and Steger, J. L.: A Numerical Simulation of Hypersonic Flows over Arbitrary Geometries at High Angle of Attack. AIAA Paper 81-0050, 1981.

6. Chaussee, D. S.; and Rizk, Y. M.: Computation of Viscous Hypersonic Flow over Control Surfaces. AIAA Paper 82-0291, 1982.

7. Schiff, L. B.; and Sturek, W. B.: Numerical Simulation of Steady Supersonic Flow over an Ogive-Cylinder-Boattail Body. AIAA Paper 80-0066, 1980.

8. Tannehill, J. C.; Venkaptapathy, E.; and Rakich, J. V.: Numerical Solution of Supersonic Viscous Flow over Blunt Delta Wings. AIAA Paper 81-0049, 1981.

9. Chaussee, D. S.; Rizk, Y. M.; and Buning, P. G.: Viscous Computations of a Space Shuttle Flowfield, Lecture Notes in Physics: Ninth International Conference on Numerical Methods in Fluid Dynamics. 218, 1984, pp. 148-153.

10. Rai, M. M.; Chaussee, D. S.; and Rizk, Y. M.: Calculation of Viscous Supersonic Flows over Finned Bodies. AIAA Paper 83-1667, 1983.

11. Chaussee, D. S.; Blom, G.; and Wai, J. C.: Numerical Simulation of Viscous Supersonic Flow Over a Generic Fighter Configuration. NASA TM-86823, 1985.

12. Wai, J. C.; Blom, G.; and Yoshihara, H.: Calculations for a Generic Fighter at Supersonic High-Lift Conditions. AGARD Fluid Dynamics Panel Symposium on Applications of Computational Fluid Dynamics in Aeronautics, France, 1986.

13. Stetson, K. F.: Experimental Results of the Laminar Boundary Layer Separation on a Slender Cone at Angle of Attack at $M_\infty = 14.2$. ARL 71-0127, 1971.

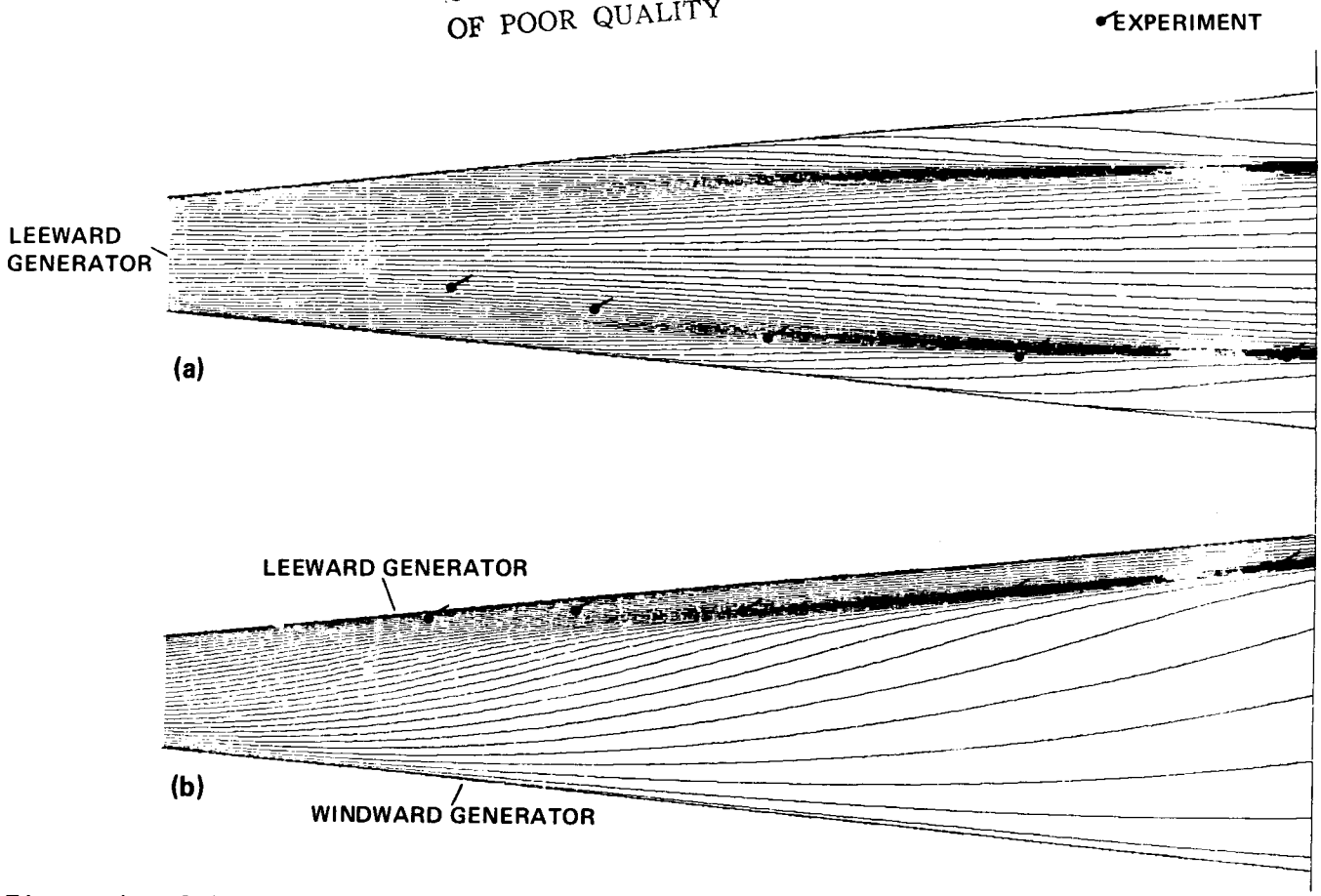

Figure 1.- Calculated limiting streamlines for flow past a sphere cone: θ_c = 5.6°; M_∞ = 14.2; Re = 6.2×10^5/ft; α = 18°. (a) Top view; (b) side view.

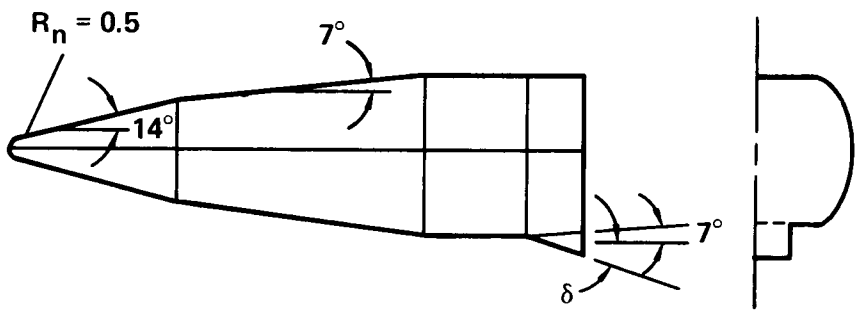

PROFILE VIEW

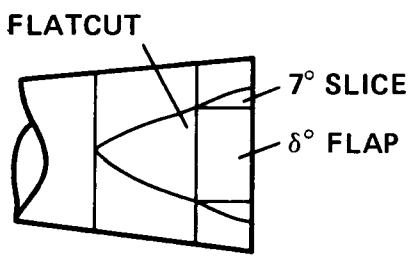

PLANFORM VIEW

Figure 2.- An MRV configuration; 14°-7° bicone.

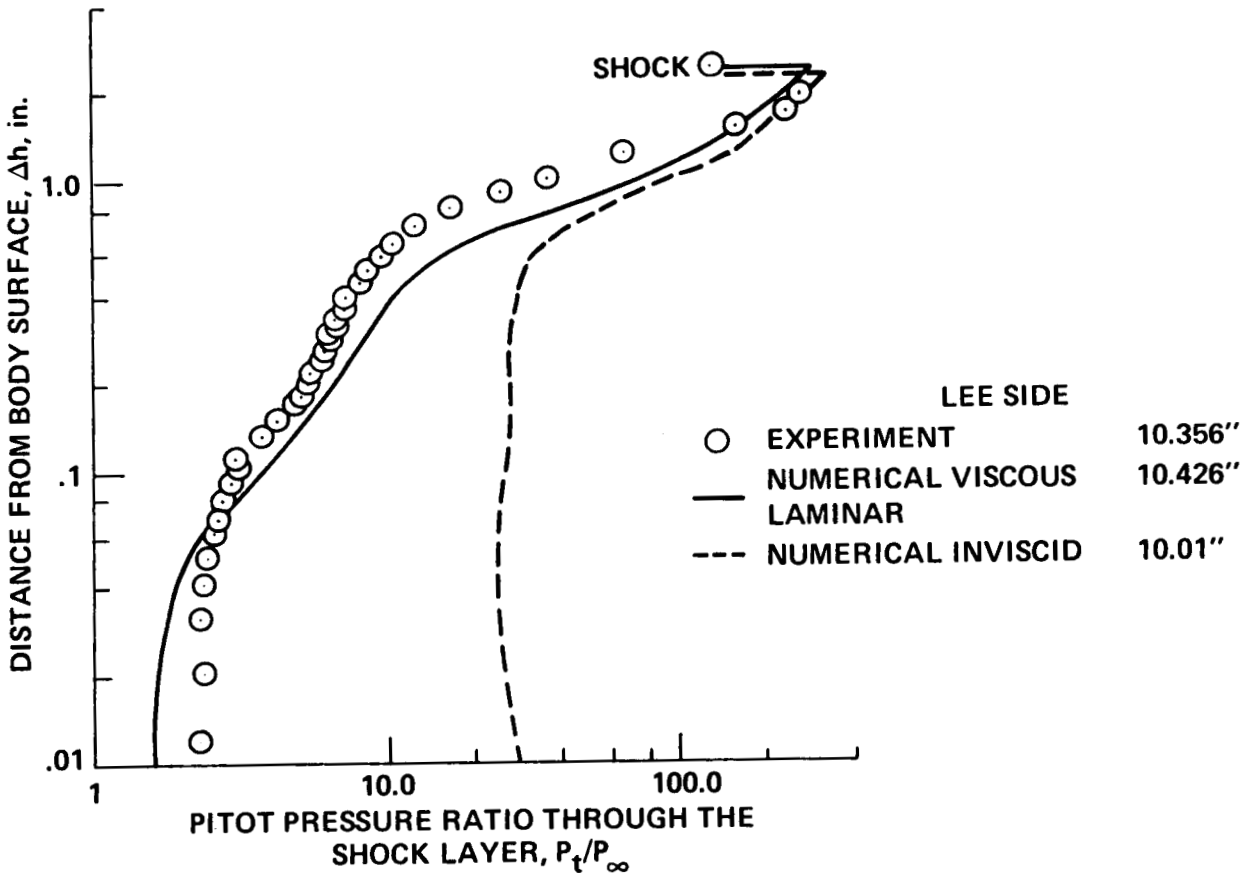

Figure 3.- Comparison between computations and experiment of the pitot-pressure variation through the shock layer: θ_c = 14°/7°; M_∞ = 10; $Re_D = 8.3\times10^4$; α = 10°; lee side X = 10.356.

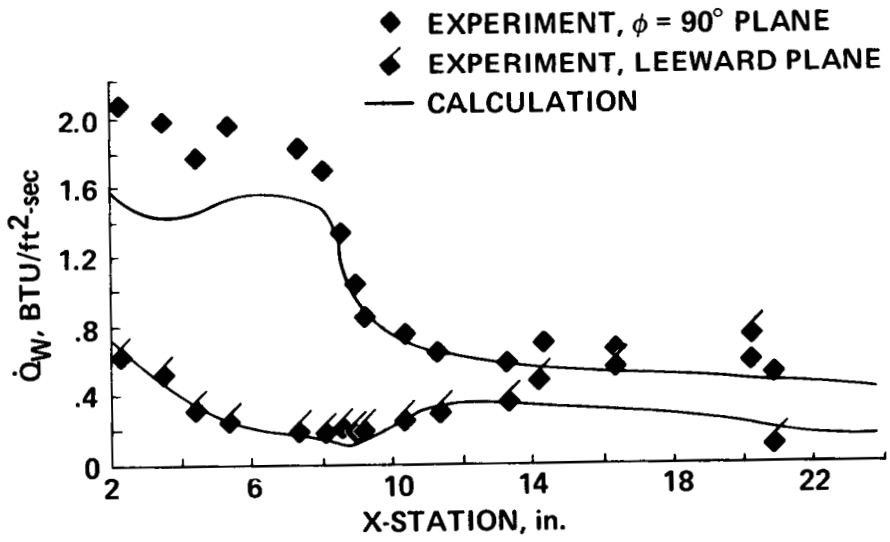

Figure 4.- Axial variation of the ϕ = 90° and the lee heat transfer: θ_c = 14°/7°; M_∞ = 10; $Re_D = 8.3\times10^4$; α = 10°.

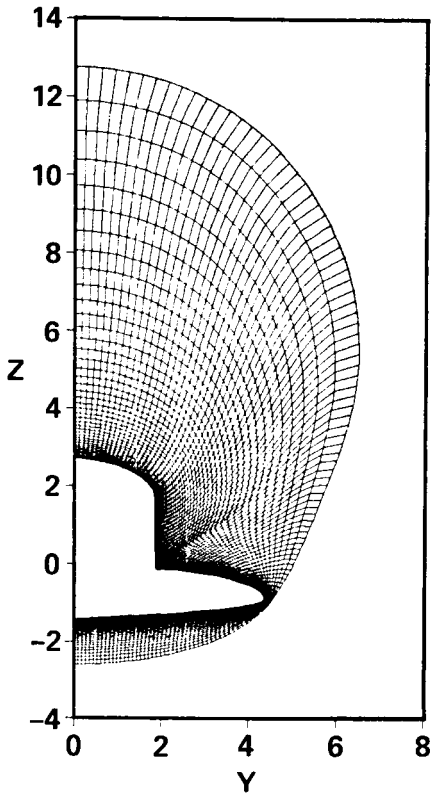

Figure 5.- Elliptic grid at X/L = 0.66.

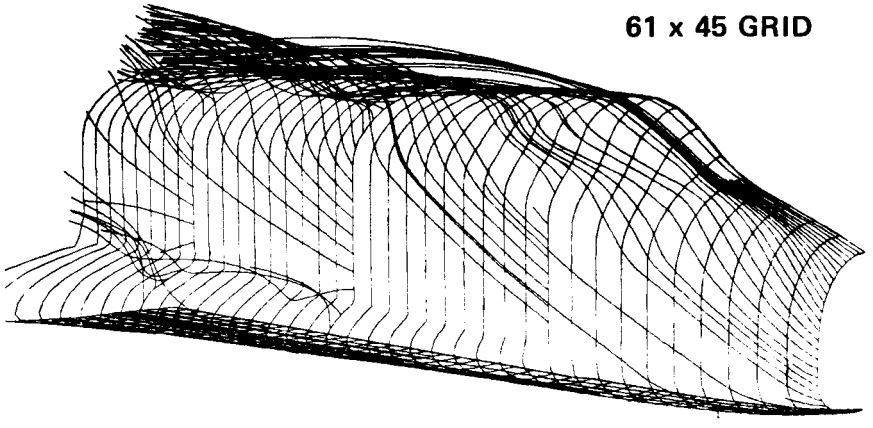

Figure 6.- Computational particle paths up to X/L = 0.66.

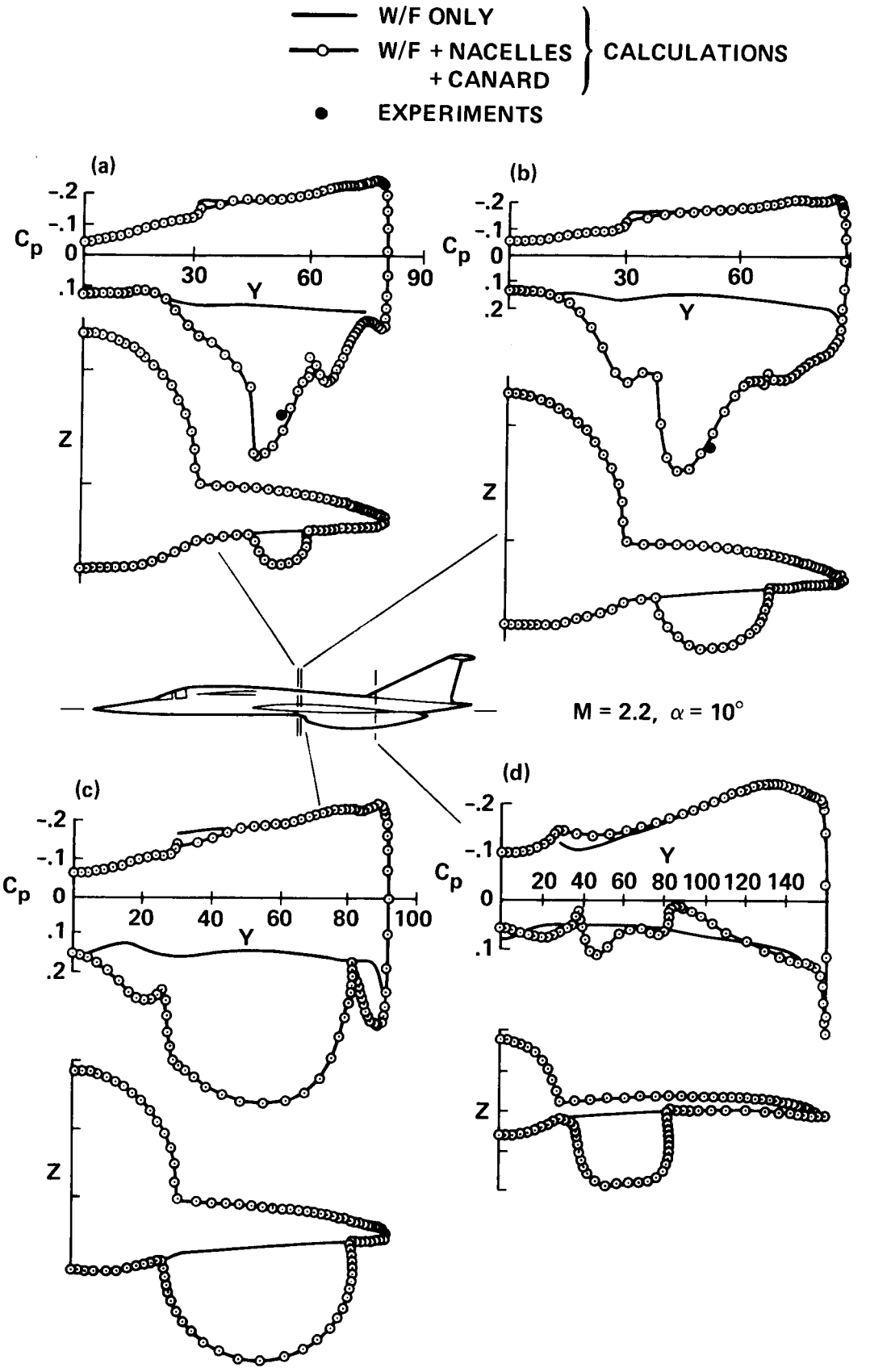

Figure 7. Cp variations at different cross-sections for wing-fuselage-nacelle at M_∞ = 2.2 and α = 10°.

NASA
National Aeronautics and Space Administration

Report Documentation Page

1. Report No.	2. Government Accession No.	3. Recipient's Catalog No.
NASA TM-100082		

4. Title and Subtitle

High-Speed Calculations Past 3-D Configurations Based on the Reynolds Averaged Navier-Stokes Equations

5. Report Date

April 1988

6. Performing Organization Code

7. Author(s)

Denny S. Chaussee

8. Performing Organization Report No.

A-88118

10. Work Unit No.

505-60

9. Performing Organization Name and Address

Ames Research Center
Moffett Field, CA 94035

11. Contract or Grant No.

13. Type of Report and Period Covered

Technical Memorandum

12. Sponsoring Agency Name and Address

National Aeronautics and Space Administration
Washington, DC 20546-0001

14. Sponsoring Agency Code

15. Supplementary Notes

Point of Contact: Denny Chaussee, Ames Research Center, MS 258-1
Moffett Field, CA 94035 (415) 694-4488 or FTS 464-4488

16. Abstract

A computational fluid dynamics tool has been developed that is capable of analyzing the viscous supersonic/hypersonic flow about realistic configurations. This technique can predict the flow in regions of canopies, wings, and canards in addition to the usual simple symmetric configurations. It also allows for interactions between aerodynamic surfaces such as the vortex interaction between canards and wings.

17. Key Words (Suggested by Author(s))	18. Distribution Statement
Computational fluid dynamics Parabolized Navier-Stokes	Unclassified-Unlimited Subject Category - 34

19. Security Classif. (of this report)	20. Security Classif. (of this page)	21. No. of pages	22. Price
Unclassified	Unclassified	11	A02